Original Article

PROGRESS in MEDICAL PHYSICS 27(3), Sept. 2016
http://dx.doi.org/10.14316/pmp.2016.27.3.117
pISSN 2508-4445, eISSN 2508-4453

Feasibility Study of Robotics-based Patient Immobilization Device for Real-time Motion Compensation

Hyekyun Chung*†, Seungryong Cho*, Byungchul Cho†

*Department of Nuclear and Quantum Engineering, Korea Advanced Institute of Science and Technology, Daejeon, †Department of Radiation Oncology, Asan Medical Center, University of Ulsan College of Medicine, Seoul, Korea

Intrafractional motion of patients, such as respiratory motion during radiation treatment, is an important issue in image-guided radiotherapy. The accuracy of the radiation treatment decreases as the motion range increases. We developed a control system for a robotic patient immobilization system that enables to reduce the range of tumor motion by compensating the tumor motion. Fusion technology, combining robotics and mechatronics, was developed and applied in this study. First, a small-sized prototype was established for use with an industrial miniature robot. The patient immobilization system consisted of an optical tracking system, a robotic couch, a robot controller, and a control program for managing the system components. A multi speed and position control mechanism with three degrees of freedom was designed. The parameters for operating the control system, such as the coordinate transformation parameters and calibration parameters, were measured and evaluated for a prototype device. After developing the control system using the prototype device, a feasibility test on a full-scale patient immobilization system was performed, using a large industrial robot and couch. The performances of both the prototype device and the realistic device were evaluated using a respiratory motion phantom, for several patterns of respiratory motion. For all patterns of motion, the root mean squared error of the corresponding detected motion trajectories were reduced by more than 40%. The proposed system improves the accuracy of the radiation dose delivered to the target and reduces the unwanted irradiation of normal tissue.

Key Words: Robotics, Mechatronics, Patient immobilizer, Respiratory motion, SBRT

Introduction

With advances in radiation techniques for imaging and therapeutic purposes, radiation treatment of cancer is becoming increasingly popular. For early-stage lung cancer in particular, stereotactic body radiation therapy (SBRT), which facilitates hypo-fractionated high-dose irradiation for tumor ablation, has been reported to yield treatment outcomes comparable to those achieved by surgery.[1] Although such a high-precision treatment requires accurate beam delivery, tumors and organs that move as a result of breathing compromise the accuracy of radiation delivery, reducing the therapeutic effects of tumor irradiation and increasing the irradiation of normal tissue. According to the Task Group 76 report[2] of the American Association of Physicists in Medicine (AAPM), developing procedures for controlling breathing-associated motion during treatment beam delivery, and incorporating this control into the treatment process, are recommended when treating thoracic/abdominal tumors such as the lung, liver, and pancreas tumors, especially if the amplitude of breathing-associated motion exceeds 5 mm.

Methods for managing respiratory motion during radiation therapy allowing the patient to breathe freely include gating techniques and real-time tumor tracking techniques. In the gating method, the treatment beam is irradiated during a specific phase of the respiratory cycle, calculated by monitoring the

This work was supported by the National Research Foundation of Korea (NRF) grant funded by the Korea government (MSIP) (No. 2015038710).
Received 31 August 2016, Revised 19 September 2016, Accepted 20 September 2016

Correspondence: Byungchul Cho (cho.byungchul@gmail.com, bcho@amc.seoul.kr)
Tel: 82-2-3010-4437, Fax: 82-2-3010-6950

breathing pattern, but this method is likely to be less accurate when the breathing pattern becomes irregular owing to prolonged treatment time.[3-6] On the other hand, with the real-time tumor tracking method the treatment time can be shorter; however, this method requires sophisticated operation and technology for changing the position and shape of the treatment beam in real time, by monitoring the three-dimensional (3D) location of a tumor. One well-known tumor tracking method uses a dynamic multi-leaf collimator (DMLC) for aligning the treatment beam to a moving tumor.[7-12] However, one problem with this approach is that the multi-leaf collimator (MLC) shapes the irradiation beam based on one-dimensional motion of individual leaves; therefore, if the tumor moves in the direction perpendicular to the direction of the leaf motion, the moving speed of the leaf must be theoretically increased or decreased indefinitely. In addition, the multi-leaf collimator is a device developed for intensity modulation of the treatment field. When leaves move continuously for beam delivery in a sliding window fashion for intensity-modulated radiation therapy (IMRT), the additional requirement to compensate for the tumor motion increases the system complexity, which inevitably reduces the accuracy and reliability of the MLC system. For these reasons, approaches that aim at decoupling the tumor motion compensation from intensity modulation, where the MLC system solely provides intensity modulation of the irradiation field, are preferred in terms of safety and efficacy of precision radiation therapy. In this regard, the Vero gimbaled linac system[13] has recently attracted attention.

Another proposed way to achieve decoupling utilizes motion compensation using couches.[14] D'Souza et al.[15] tested the Hexapod for this purpose and concluded that a low speed limit of 8 mm/s was insufficient for ensuring effective respiratory motion compensation. In the present study, we aimed to develop an alternative robotic patient immobilization system that can compensate the tumor motion in real time. By combining a robotic arm with six degrees of freedom (DOF) and a patient positioning couch, a control system has been developed for monitoring the target location in real time and for computing the compensatory motion of the robot couch. First, the system was evaluated by considering a prototype system and control algorithms, in a miniaturized test environment. Then, we tested our system on a full-scale robot couch, to evaluate the applicability and limitations of the robot couch technology in real-time tumor tracking radiation therapy.

Materials and Methods

1. System configuration

The prototype patient immobilization system and the flow chart of the process of motion compensation using the system are shown in Fig. 1. The prototype system was miniaturized and consisted of an industrial 6-axis jointed-arm robot manipulator (HA006-04, Hyundai Heavy Industries Co., Ltd., Korea), a couch on the robotic arm, an optical tracker, and a robot controller connected to a personal computer (PC) for controlling the integrated system. The system was constructed to be movable. The weight capacity of the industrial 6-axis vertical articulated robot was 6 kg. The mechanical parameters and specifications of the HA006-04 robot are summarized in Table 1. A miniaturized couch for patient support was connected to

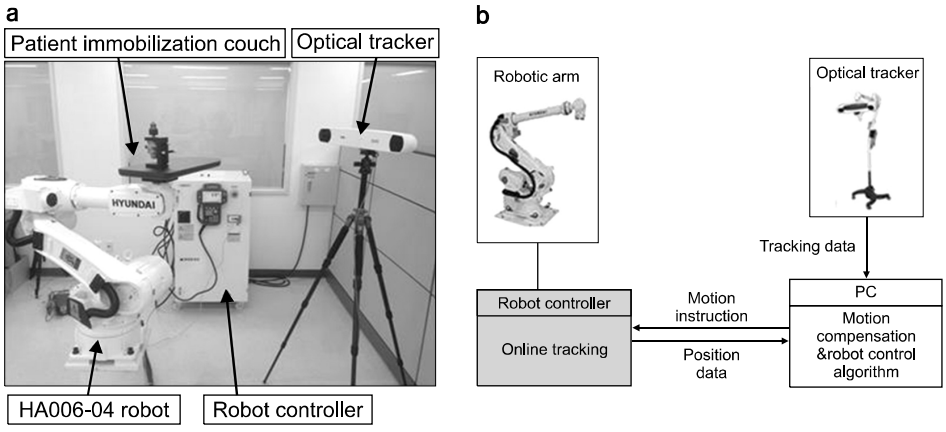

Fig. 1. (a) Prototype of the patient immobilization system consisting of a robotic arm, a couch, a robot controller, an optical tracker, and a camera. (b) Schematic of the motion compensation system.

Table 1. Mechanical specifications and limitations of the two robot manipulators used in this study.

			HA006A-04	HS160L
Payload			6 kg	160 kg
Max. reach			1,425 mm	3,036 mm
Degree of freedom			6 Axes	6 Axes
Max. motion range	S	Swivel	±172°	±180°
	H	For/Backward	+180°~−78°	+180°~−65°
	V	Up/Downward	+180°~−82°	+230°~−135°
	R2	Rotation 2	±180°	±360°
	B	Bending	±135°	±130°
	R1	Rotation 1	±360°	±360°
Max. speed	S	Swivel	230°/s	95°/s
	H	For/Backward	230°/s	95°/s
	V	Up/Downward	230°/s	95°/s
	R2	Rotation 2	430°/s	150°/s
	B	Bending	430°/s	145°/s
	R1	Rotation 1	640°/s	220°/s
	R2	Rotation 2	1.2 kgf.m	105 kgf.m
	B	Bending	1.0 kgf.m	105 kgf.m
	R1	Rotation 1	0.6 kgf.m	50 kgf.m
Repeatability			±0.04 mm	±0.15 mm
Approximate weight			150 kg	985 kg
Max. rated power			4.4 kVA	8 kVA
Controller model			Hi5a	Hi5a

the flange of the robot manipulator. The industrial robot controller used in this study is shown in Fig. 1(a) (Hi5-N30, Hyundai Heavy Industries Co., Ltd., Korea). The robot controller operated based on the teaching-and-playback method. A point-to-point interpolation, linear interpolation, and circular arc interpolation were also possible in the controller. The robot controller received external commands via an Ethernet protocol, including commands related to the destination position and direction.

The couch for the phantom or patient support and immobilization was made of carbon fiber reinforced plastic (CFRP). The miniaturized couch for the prototype system was 600 mm long. CFRP is a lightweight structural material, characterized by high strength and high elasticity. Although the specific strength of CFRP is six times higher than that of steel, radiation transmission through a CFRP couch can be high, owing to a low-density foam filling covered by a sheet of CFRP. For these reasons, CFRP is commonly used in patient support couches and immobilization devices in radiation therapy. To improve the accuracy of the radiation treatment, radiation penetrability of a patient supporter or immobilizer is required for minimizing the disturbance to beam delivering. According to the AAPM Task Group 176 report,[16] CRFP couches can increase the skin irradiation dose rate to 40~80% of the maximal absorbed dose, while the original skin irradiation dose rate is 20%. Meanwhile, the intensity reduction ratio of CRFP for a 6 MV beam is ~2%, which is within acceptable ranges. Moreover, the effects of CFRP couches on beam delivery can be processed appropriately in treatment planning systems (TPS). Consequently, in the present study the patient support couch was manufactured using CFRP. A silicone rubber damper was added to the fixation part of the couch for reducing and absorbing the couch vibration. The material for the fixation part was aluminum, which is lightweight.

The controller PC calculated and sent increments of position values for motion compensation, based on the patient position data collected by the optical tracker. An industrial PC was used as a controller PC owing to its stability and the possibility to incorporate additional input/output (I/O) systems. The operating systems on the controller PC were Windows 7 (Microsoft, USA) and RTX (Intervalzero, USA). RTX is a real-time operating system for transmission of equidistant inter-

vals of robotic control signals. Shared memory between Windows 7 and RTX was used for sharing the data required for controlling the robot. Input and output data processing and user interface were implemented on the Windows 7 platform, while calculation of the position data and data transmission to the robot controller were implemented on the RTX platform. The patient motion compensation data were transmitted using the user datagram protocol (UDP). For motion compensation commands, coordinates in the optical tracker coordinate system were transformed into the robot system coordinates.

An optical 3D marker position tracker (Polaris Spectra, NDI, Canada) was used for data generation and for position detection. Passive type infrared reflecting markers were attached to the target and the optical tracker detected the markers' positions. The marker position data, with three DOF, were extracted from the marker shapes, locations, and directions. The root mean squared (RMS) error of the target position detection using the Polaris optical tracker was 0.25 mm. The sampling frequency of the target position detection system was 30 Hz. The maximal data transmission speed between the tracker and the controller PC was 1.2 Mbps, and the data were transmitted via a universal serial bus (USB) cable. The range of the tracking area was at most 2,400 mm (3,000 mm for special options) and the area was pyramid-shaped.

2. Motion compensation system

Before using the system for real-time robotic motion compensation, we performed preliminary processing and testing, including calibration of the system and transformation of coordinates. Before performing position measurements, mechanical parameters need to be corrected by the system geometric calibration, to enable high-precision motion control. The geometric calibration was performed by measuring the markers' positions for 27 different directions and positions. After the mechanical parameter correction for geometric calibration, we verified the system geometric accuracy by measuring position errors for eight different points in space, for different couch orientations.

Subsequently, the transformation between the robot coordinate system and the optical tracker coordinate system was measured and calculated for matching the position data across the robot and the optical tracker. Because the robot and the tracker coordinate systems are different, coordinates in motion compensation commands issued to the robot had to use the robot coordinate system. To determine the transformation of coordinates, eight different positions with the same couch orientation were provided to the robot controller and were detected by the optical tracker. Then, a 4×4 transformation matrix R was calculated by minimizing the error between the positions' coordinates in the robot coordinate system and the coordinates reported by the optical tracker in the tracker coordinate system.

The input position data to the robot controller were generated from a sample patient motion data. The sample motion data were organized in terms of the displacement values for x, y, and z, in millimeters, sampled with a frequency of 50 Hz. The input motion data were generated by sampling the position data from a 60-s-long window, with a sampling frequency of 10 Hz. From the extracted motion data, several job files were created as a possible input to the robot controller. Although position and direction data with six DOF could be provided to the robot controller, in practice we only controlled three DOF in the position data in the present study.

3. Patient-scale system configuration

After developing the prototype motion compensation system with the miniature couch and robot, we scaled the system to realistic clinical dimensions, considering a larger robot manipulator and a patient support couch as in Fig. 2. The robot manipulator used for this enlarged system was an HS160L industrial 6-axis vertical articulated robot (Hyundai Heavy Indus-

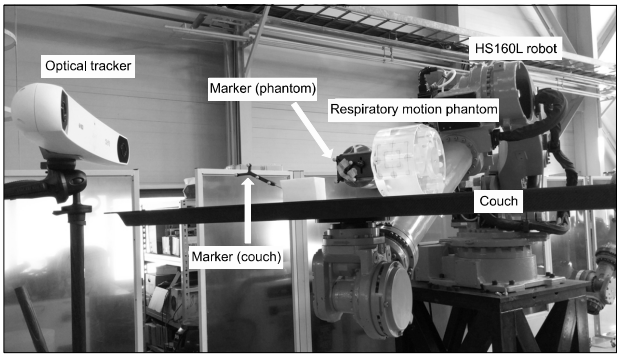

Fig. 2. Real-scale patient immobilization system for evaluating the motion compensation performance with respect to the respiration-associated motion.

tries Co., Ltd., Korea), with 160 kg weight capacity. The mechanical parameters and the specifications of the HS160L model are listed in Table 1. The real-scale couch was 2 m long and was made of CFRP, the same as the prototype couch. The robot controller, the system control PC, and the optical tracker were the same as those used in the prototype system.

4. Motion compensation implementation and evaluation

The program for motion control was written in C++, and a screenshot of the control window is shown in Fig. 3(a). The data flow and data processing algorithm is listed in Fig. 3(b). Upon receiving position data from the optical marker tracker, the control program calculated the prediction for position data in the next time step. Subsequently, the program issued commands to the robot controller to generate equal and opposite displacement to the predicted one, for offsetting the anticipated displacement in the next time step. Before issuing these displacement commands, the coordinates were converted from the optical tracker system to the robot system of coordinates.

Next, we used a dynamic motion phantom to evaluate the performance of the developed motion compensation system. First, to measure the delay time of the robot reaction, the robot was commanded to track uniform circular motion of the dynamic phantom isolated from the patient immobilization system. The positions of two optical markers on the couch and the phantom were tracked simultaneously using the 3D optical tracker. Then, the average temporal difference between two trajectory data was measured.

For measuring the motion compensation accuracy, a respiratory motion phantom (Quasar, Modus Medical Devices, Canada) was used to realistically mimic respiratory motion patterns. Several one-dimensional motion patterns from real patients were applied to the phantom. For evaluating the prototype system, seven types of respiratory motion, including typical, typical-fast, typical-slow, irregular, drift-artifact, cardiac-artifact, and jitter-artifact patterns were used. For the enlarged real-scale system, only typical, typical-slow, and irregular respiratory motion patterns were used because this was deemed to be meaningful based on the experiments with the prototype system.

Results

1. Measurement data of robot motion

For the robot calibration and for validating the extent of precision of the robot mechanical parameters, we measured position data of the markers on the couch for 8 points in space, for different couch orientations. As is evident from Table 2,

Table 2. Calibration errors between the input positions to the robot and the measured positions.

Point number	Error (mm)
1	0.07
2	0.10
3	0.08
4	0.07
5	0.10
6	0.08
7	0.10
8	0.06
Average	0.08

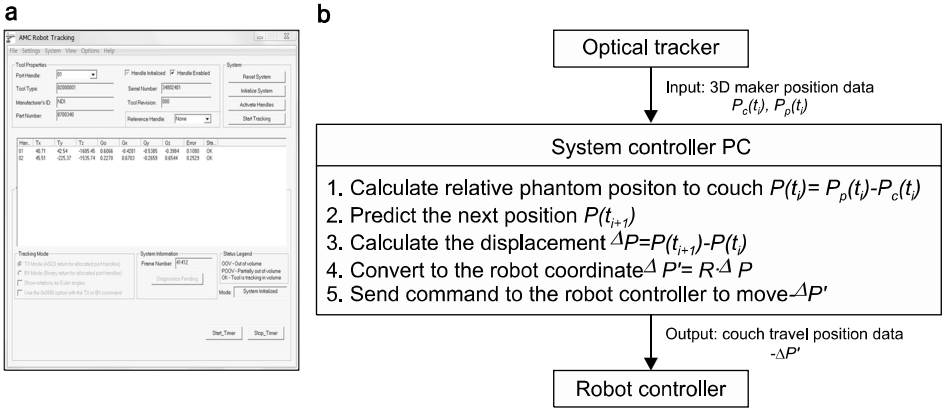

Fig. 3. (a) Screenshot of the in-house motion detection and control program running on the system control PC. (b) Algorithm flow chart of the developed motion compensation system. $P_c(t_i)$ and $P_p(t_i)$ are 3D positions of the marker on the couch and the marker on the motion phantom at time t_i. R is the coordinate transformation matrix, from the optical tracker system of coordinates to the robot system of coordinates.

for each detection point the average robot position error was 0.08 mm. Consequently, the robot position calibration was considered to be sufficiently precise.

Using the coordinate transformation matrix, the average discrepancy between the position data detected by the optical tracker and the data provided to the robot was 0.18 mm. The inputted robot positions and the transformed optical positions are listed in Table 3.

2. Evaluation of temporal delay and performance of motion compensation

The measured average temporal delay of the prototype robot reaction was 200 ms, regardless of the motion direction. For the real-scale system, the average temporal delay increased to 350 ms for all directions. In Fig. 4, the motion compensation results are shown for the prototype system (a) and for the real-scale system (b) with the typical-slow respiratory motion pattern applied to the Quasar dynamic phantom. In the first half of the measurement process, motion compensation was not applied. Therefore, only the target position on the phantom (red line) moved along the patient respiratory trajectory (blue line) inputted to the phantom, while the robot couch position (green line) was stationary, as seen for the first halves of all trajectories in Fig. 4. Motion compensation was applied during the second half of the measurement process. The target phantom motion range (red line) was reduced after applying the

Table 3. Input position data provided to the robot and the measured positions in the robotic coordinate system.

Point number	Robot input positions			Converted measurement positions		
	X (mm)	Y (mm)	Z (mm)	X (mm)	Y (mm)	Z (mm)
1	310	0	870	310.10	0.12	870.08
2	410	0	870	410.07	−0.03	869.85
3	360	200	870	359.96	199.61	869.95
4	410	200	970	409.94	199.66	969.96
5	310	−200	870	310.09	−199.62	870.08
6	410	−200	870	409.92	−199.82	869.92
7	410	−200	970	410.05	−199.85	970.04
8	410	0	970	409.87	−0.08	970.12

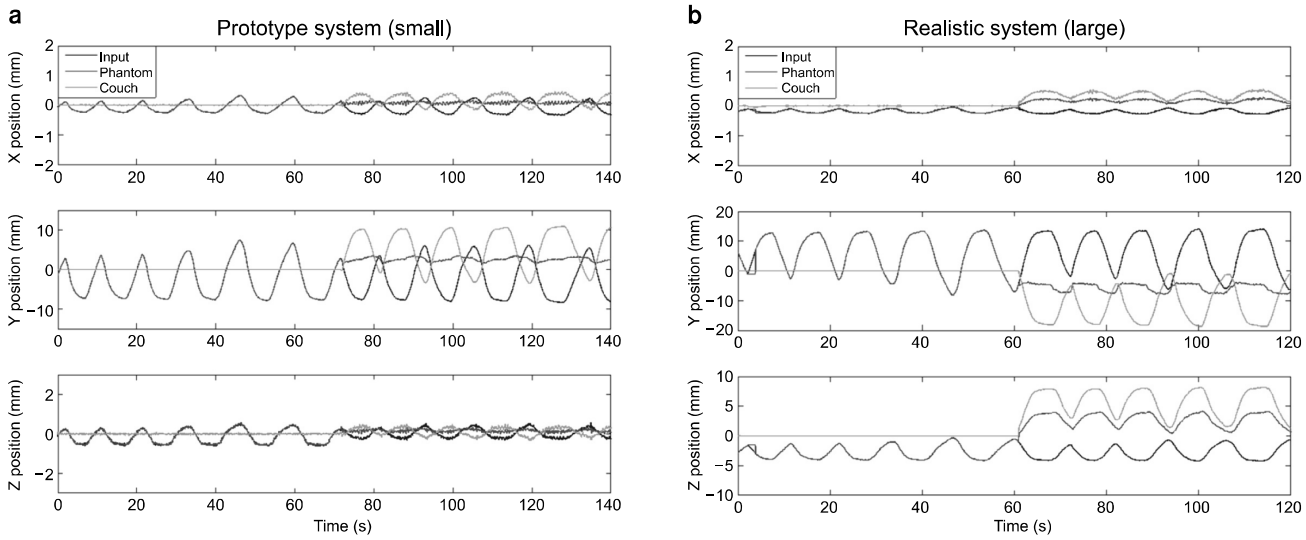

Fig. 4. 3D position data measured by the optical tracker, for markers attached to the motion phantom and couch. The typical-slow respiratory motion pattern was considered here. (a) Results obtained for the prototype system. (b) Results obtained for the real-scale system. The motion compensation was initiated about halfway into the measurement period.

motion compensation, while the couch (green line) moved in the opposite direction to that of the phantom, as shown in the second halves of the trajectories. Tables 4 and 5 list the 3D RMS errors (RMSEs) before and after applying the motion compensation, as well as the reduction ratios of the 3D RMSE for the prototype system and for the real-scale system. For the prototype system, the 3D RMSE reduction ratio was 55% to 89% after applying motion compensation, for all types of respiratory patterns. For the real-scale system, the 3D RMSE reduction ratio was 40% to 70% after applying motion compensation. The performance of the motion compensation was respiratory pattern-dependent. The most significant reduction in the error was observed for the typical-slow respiratory pattern, while the motion compensation was less effective for fast motion or motion containing artefacts.

Discussion and Conclusion

In this study, as an interim stage, a miniaturized mobile robotic couch system, characterized by ease of access and control, was used for developing an integrated control system and for determining its feasibility. The developed control system, based on the miniaturized system, was confirmed to be equally applicable to a full-size robot couch system, except that the delay time of the real-scale system response increased 1.5-fold, owing to a relatively large size of the real-scale system. The two systems (miniature and full-scale) performed equally well in terms of their driving mechanism, control algorithm, and operating environment. Longer reaction time in the larger system is apparently caused by a heavier burden on the 6-axis joint robot arm, owing to a heavier weight. Therefore, reaction time should be determined for a situation in which the weight of the patient is fully loaded on the patient supporting couch system. The development and application of the motion prediction algorithm to the motion compensation control program can prevent a reduction in the position determination accuracy by effectively compensating the response delay. In this case, simply adjusting the delay time according to the weight loading is expected to yield the same correction accuracy and efficiency.

Although the larger robot used in this study is difficult to access and move, it is possible to incorporate the full-scale robotic couch system developed in this study into the actual treatment room environment in the future. However, since this study has confirmed that there is no significant difference between the two scale systems, it is preferred to conduct additional investigations using the smaller system, and then fine-tune the relevant control parameters in the full-scale system.

In this study, we only considered the couch movement with three DOF, i.e., the 3D translational motion of the robot couch was incorporated into the design of the computerized robot couch. However, according to a study involving 40 patients, in which a six DOF computerized robotic couch was used for the patients' setup during brain cancer SBRT, average rotation errors of $0.23^{o}\pm0.82^{o}$ (longitudinal), $-0.09^{o}\pm0.72^{o}$ (lateral), and $-0.10^{o}\pm1.03^{o}$ (vertical) were obtained.[17] In addition, according to another study involving 29 patients, in which position changes of implanted markers were measured in liver SBRT, the average range (2～98 percentile) of the translational/rotational motion was 2.0 mm/3.9° (right-left), 9.2 mm/2.9° (superior-inferior), 4.0 mm/4.0° (anterior-posterior), and 10.5

Table 4. 3D RMSEs, before and after applying the motion compensation, and the reduction ratios of the 3D RMSEs for seven motion patterns measured using the small-scale prototype device.

Motion pattern	3D RMSE	3D RMSE (Compensated)	Error reduction ratio (%)
Typical	4.01 mm	1.52 mm	62.2
Typical-fast	4.48 mm	2.30 mm	48.7
Typical-slow	4.70 mm	0.51 mm	89.1
Irregular	3.06 mm	1.35 mm	55.9
Drift-artifact	3.27 mm	1.46 mm	55.4
Cardiac-artifact	2.25 mm	1.24 mm	44.9
Jitter-artifact	3.26 mm	1.50 mm	54.1

Table 5. 3D RMSEs, before and after applying the motion compensation, and the reduction ratios of the 3D RMSEs for three motion patterns measured using the real-scale device.

Motion pattern	3D RMSE	3D RMSE (Compensated)	Error reduction ratio (%)
Typical	5.63 mm	2.95 mm	47.7
Typical-slow	6.54 mm	1.77 mm	72.9
Irregular	3.94 mm	2.35 mm	40.4

mm in three dimensions, and the error was reduced in half by correcting the rotational motion.[18] Therefore, the robot motion compensation treatment units should be designed to provide motion with six DOF, consisting of three-axis translational motion and three-axis rotational motion.

In the present study, we developed a robotic couch control system using industrial robot systems for real-time respiratory tumor motion compensation during radiation therapy. As an interim stage, a miniaturized test model was used to provide a preferential environment for developing and testing the control driver system, following which the same control system was tested on a full-scale system. In real-time tumor tracking experiments, using a three DOF respiratory motion phantom the demonstrated compensation efficiency exceeded 40%. In this study, we focused only on the geometrical accuracy due to the respiratory tumor motion, with and without couch tracking. However, the dosimetric impact of the geometric errors is the most relevant issue for estimating clinical implications. Therefore, additional quantitative analysis of dosimetric impact has to be performed on several variables, such as the delay time, beam energy (6/15 MV), treatment delivery (3D/4D), treatment type (conformal/IMRT), beam direction (AP/PA), and breathing training type (free breathing/audio instruction/visual feedback). Nonetheless, further development of the prototype robot couch system proposed in this study is expected to improve the precision of treatment and thus to further alleviate the treatment side effects.

References

1. Timmerman RD: Surgery versus stereotactic body radiation therapy for early-stage lung cancer: Who's down for the count? J Clin Oncol 28(6):907-909 (2010)
2. Keall PJ, Mageras GS, Balter JM, et al: The management of respiratory motion in radiation oncology report of AAPM Task Group 76. Med Phys 33(10):3874-3900 (2006)
3. Ohara K, Okumura T, Akisada M, et al: Irradiation synchronized with respiration gate. Int J Radiat Oncol Biol Phys 17(4):853-857 (1989)
4. Kubo HD, Hill BC: Respiration gated radiotherapy treatment: a technical study. Phys Med Biol 41(1):83-91 (1996)
5. Ford EC, Mageras GS, Yorke E, Rosenzweig KE, Wagman R, Ling CC: Evaluation of respiratory movement during gated radiotherapy using film and electronic portal imaging. Int J Radiat Oncol Biol Phys 52(2):522-531 (2002)
6. Vedam SS, Keall PJ, Kini VR, Mohan R: Determining parameters for respiration-gated radiotherapy. Med Phys 28(10):2139-2146 (2001)
7. Schweikard A, Shiomi H, Adler J: Respiration tracking in radiosurgery. Med Phys 31:2738-2741 (2004)
8. Murphy MJ: Tracking moving organs in real time. Semin Radiat Oncol 14(1):91-100 (2004)
9. Keall PJ, Kini VR, Vedam SS, Mohan R: Motion adaptive X-ray therapy: a feasibility study. Phys Med Biol 46(1):1-10 (2001)
10. Cho B, Poulsen PR, Sawant A, Ruan D, Keall PJ: Real-time target position estimation using stereoscopic kilovoltage/megavoltage imaging and external respiratory monitoring for dynamic multileaf collimator tracking. Int J Radiat Oncol Biol Phys 79(1):269-278 (2011)
11. Fledelius W, Keall PJ, Cho B, et al: Tracking latency in image-based dynamic MLC tracking with direct image access. Acta Oncol 50(6):952-959 (2011)
12. Poulsen PR, Cho B, Sawant A, Keall PJ, et al: Implementation of a new method for dynamic multileaf collimator tracking of prostate motion in arc radiotherapy using a single kV imager. Int J Radiat Oncol Biol Phys 76(3):914-923 (2010)
13. Depuydt T, Poels K, Verellen D, Engels B, et al: Treating patients with real-time tumor tracking using the Vero gimbaled linac system: implementation and first review. Radiother Oncol 112(3):343-51 (2014)
14. Lee S, Chang KH, Shim JB, Cao Y, et al: Evaluation of mechanical accuracy for couch-based tracking system (CBTS). J Appl Clin Med Phys 13(6):157-169 (2012)
15. D'Souza WD, Naqvi SA, Yu CX: Real-time intra-fraction-motion tracking using the treatment couch: a feasibility study. Phys Med Biol 50(17):4021-33 (2005)
16. Olch AJ, Gerig L, Li H, Mihaylov I, Morgan A: Dosimetric effects caused by couch tops and immobilization devices: report of AAPM Task Group 176. Med Phys 41(6):061501-1-30 (2014)
17. Gevaert T, Verellen D, Engels B, et al: Clinical evaluation of a robotic 6-degree of freedom treatment couch for frameless radiosurgery. Int J Radiat Oncol Biol Phys 83(1):467-474 (2012)
18. Bertholet J, Worm ES, Fledelius W, Høyer M, Poulsen PR: Time-resolved intrafraction target translations and rotations during stereotactic liver radiation therapy: implications for marker-based localization accuracy. Int J Radiat Oncol Biol Phys 95(2):802-809 (2016)